



HAL
open science

Conjugate Mixed Convection in a Horizontal Cylindrical Duct under the Solid Shell Internal Heat Generation

Rachid Bessaih, Chérifa Abid

► **To cite this version:**

Rachid Bessaih, Chérifa Abid. Conjugate Mixed Convection in a Horizontal Cylindrical Duct under the Solid Shell Internal Heat Generation. *Journal of Applied and Computational Mechanics*, 2021. hal-03658267

HAL Id: hal-03658267

<https://amu.hal.science/hal-03658267>

Submitted on 3 May 2022

HAL is a multi-disciplinary open access archive for the deposit and dissemination of scientific research documents, whether they are published or not. The documents may come from teaching and research institutions in France or abroad, or from public or private research centers.

L'archive ouverte pluridisciplinaire **HAL**, est destinée au dépôt et à la diffusion de documents scientifiques de niveau recherche, publiés ou non, émanant des établissements d'enseignement et de recherche français ou étrangers, des laboratoires publics ou privés.

HEAT TRANSFER ANALYSIS FOR MIXED CONVECTION IN A HORIZONTAL CYLINDRICAL DUCT

Rachid Bessaïh^{1*} and Chérifa Abid²

¹Laboratoire LEAP, Département de Génie Mécanique,
Université Frères Mentouri-Constantine 1, Route de Ain El. Bey, Constantine 25000, Algérie.

²Aix-Marseille Université, CNRS, IUSTI UMR 7343, 5 rue Enrico Fermi, 13453 Marseille Cedex 13, France.

*Corresponding author: bessaïh.rachid@gmail.com ; Phone/Fax: +213 31 81 13 03

Received January 15 20xx; Revised March 20 20xx; Accepted for publication June 20 20xx.

Corresponding author: Saliha Bellout, belloutsaliha@gmail.com

© 2018 Published by Shahid Chamran University of Ahvaz

& International Research Center for Mathematics & Mechanics of Complex Systems (M&MoCS)

Abstract. This paper deals with three-dimensional, mixed convection in a cylindrical duct horizontally. This latter is partially subjected to a uniform volumetric heat generation at the solid-liquid interface. The working fluid (water) with a parabolic velocity profile and a constant temperature T_0 enters the tube. The study was carried out for different Richardson numbers values $Ri=0.1-8$ at Reynolds number $Re=600$. Results were conducted so that to show the influence of Richardson number Ri on the dynamic and thermal fields and local Nusselt number $Nu(\theta,z)$ and peripherally averaged axial Nusselt number $Nu(z)$. Also, analyses of the results showed that the hydrodynamic effects are manifested by the existence of secondary flow, inducing temperature gradient at a cross-section between the top and bottom of the duct. The reversed flow is observed for a low Reynolds number $Re=10$. A significant increase in heat exchange is observed in mixed convection compared to pure forced convection flow. Correlations for the variation of average Nusselt number $Nu(Ri,z)$ at the entrance region with Ri and $z=z'/Di$ and local Nusselt $Nu(Ri)$ number in the hydrodynamics establishment zone are proposed and compared with the present numerical results.

Key words: Mixed convection, heat transfer, horizontal duct, local and average Nusselt numbers

Nomenclature

Di	internal duct diameter, m
Do	external duct diameter, m
e	thickness of the duct, m
g	acceleration of gravity, m/s^2
Gr	Grashof number
h	convective heat transfer coefficient, $W/m^2.K$
h_r	radiative heat transfer coefficient, $W/m^2.K$
I	current density, A
k	thermal conductivity, $W/m.K$
k^*	dimensionless thermal conductivity
L	length of the duct, m
$Nu(\theta,z)$	local Nusselt number
$Nu(z)$	peripherally averaged axial Nusselt number
P	dimensionless pressure
Pr	Prandtl number
q_v	rate of energy generation per volume unit, W/m^3
r	non-dimensional radial coordinate
r'	dimensional radial coordinate, m
Re	Reynolds number

Greek symbols

α	fluid thermal diffusivity, m^2/s
β	coefficient of thermal expansion, K^{-1}
ε	emissivity coefficient
Θ	non-dimensional temperature
ν	fluid kinematic viscosity, m^2/s
ν^*	non-dimensional kinematic viscosity
θ	angular coordinate, rad
ρ	density of the fluid, kg/m^3
σ	Stephan-Boltzmann constant, $\sigma=5.67 \times 10^{-8} W/m^2 K^4$

Subscripts

f	fluid
m	mean value
s	solid
w	wall

S	non-dimensional source term
T	temperature, K
u	dimensionless radial velocity
v	non-dimensional axial velocity
w	non-dimensional azimuthal velocity
z	non-dimensional axial coordinate
z'	dimensional axial coordinate, m

1. Introduction

Heat transfer with mixed convection in ducts is of great interest for industrial applications like heat exchangers, cooling of nuclear reactors, solar collectors, geothermal power generation, the food, and biomedical industries...etc...

Mixed convection was the topic of many theoretical, experimental, and computational studies in pipes. For example, Abid et al.[1] investigated mixed convection in a long heated horizontal cylindrical duct using analytical and numerical approaches. The wall temperature was experimentally determined by infrared thermography. Results show the hydrodynamic establishment of a secondary flow characterized by the presence of two counter-rotating transverse rollers. Besides, the thermal establishment is characterized by an increase in the mean temperature of the cylinder wall. K.Choi and H. Choi [2] have shown the increase in heat exchange and the appearance of natural convection rolls, related to the establishment of mixed convection inside a non-uniformly heated horizontal tube on its circumference. Hwang et al.[3] studied numerically mixed convection within a cylindrical horizontal duct. A correlation was obtained giving Nu with Ra. Ouzzane and Galanis [4] analyzed the effects of parietal conduction and heat flow distribution on laminar mixed convection inside a conduit inclined for four different thermal boundary conditions. They illustrated the effects on conjugated transfer flow and non-uniform heating conditions. Habib et Negm[5] presented a numerical analysis on steady laminar mixed convection in a concentrated horizontal annulus with non-uniform circumferential heating. Results suggested that the effects of buoyancy on the mixed convection are clearly sensitive to heaters. Orfi and Galanis[6] were interested in the effects on flow, thermal, and concentration fields of the solutal and thermal Grashof numbers in horizontal and vertical tubes. Results show the influence of the Grashof number and the inclination of the tube on the flow field. The effect of the Lewis number on laminar mixed convective heat and mass transfer in a horizontal tube with uniform heat flux and concentration was investigated numerically by Orfi and Galanis[7]. The authors concluded that the impact of Lewis number on the number of Sherwood is greatest near tube entrance.

Mohammed and Selman [8] experimentally approached laminar heat transfer with mixed convection for airflow in a cylindrical duct tilts for different Re values, heat flux, and inclination angle. They deduced that the surface temperature along the duct, local Nusselt number distribution according to dimensionless axial distance ($x/D.Re.Pr$). They have also found that if the heat flow increases for the same Re, the surface temperature increases. Correlations that give Nu based on Ra for three inclinations were obtained. In Mohammed and Salman's experimental work on mixed convection in a horizontally oriented cylinder [9], authors were able to conclude that free convection reduces heat transfer for a small Reynolds number ($Re = 400$) and increases heat transfer for $Re = 1600$. Mohammed and Salman [10-13] performed experimental work on natural and forced convective heat transfer in both vertical and horizontal circular cylinders. For example, in [10], the average heat transfer results were correlated with the empirical correlation, and an increase in the Nu values as the heat flux rises was observed in [11] for all entrance sections.

The effect of geometric parameters on laminar mixed convection in an inclined eccentric straight annulus was investigated numerically by Shiniyan et al.[14]. Results showed that for an angle of inclination equal to 55° , Nu has the maximum value. Testi[15] measured heat transfer coefficients at six cross-sections along the uniformly heated horizontal cylindrical pipe under transitional mixed convection; for the entire heat transfer surface, a single Nusselt number correlation was proposed. Chae and Chung [16] performed experimentally mixed convection in horizontal pipes for different values of Gr and Re.

A correlation was developed using a semi-empirical buoyancy coefficient. Schriener and El-Genk[17] performed a numerical analysis of turbulent heat transfer by convection in a uniformly heated circular tube. The average Nusselt numbers for fully developed flows are correlated with Peclet number. Colombo *et al.* [18] studied numerically heat transfer by mixed convection in a uniformly heated concentric annulus. Results show that mass flow reduction is affected by axial shear stress. In a horizontal duct, Ganesan et al.[19] conducted a numerical analysis of mixed convection heat transfer with radiation. Results show that average Nu is influenced by flow conditions and surface radiation.

The present work deals with laminar mixed convection in a long, uniformly heated, horizontal duct at the wall. The fluid employed is water. The effect of Ri on the fluid flow, thermal field, $Nu(\theta, z)$, and $Nu(z)$ have been investigated numerically.

To the literature relevant, there are very few experimental or numerical works, showing the variation of $Nu(z)$ in the entry region and $Nu(\theta, z)$ along the peripheral wall. The study focuses on heat transfer, including the variation of average and local Nusselt numbers.

This paper is structured according to the following. Section 2 provides a description of the geometry and the governing equations with boundary conditions. The numerical approach and code validation are discussed in Section 3. Section 4 describes the results and discussions.

2. Geometry description and governing equations

2.1 Geometry description

Figure 1 depicts the geometry under consideration. A horizontal cylinder having a length $L=100\text{cm}$, an internal diameter $D_i=1\text{cm}$ and an external diameter $D_o=1.04\text{cm}$, is made of Inconel (thermal conductivity $k_s=20\text{W/m.K}$). An electric current I produces a rate of energy generation per unit volume q_v by Joule effect along with the thickness of the wall $e=0.2\text{ cm}$. At the inlet duct, the axial velocity v of the water flow has a parabolic profile and the fluid is held at $15\text{ }^\circ\text{C}$.

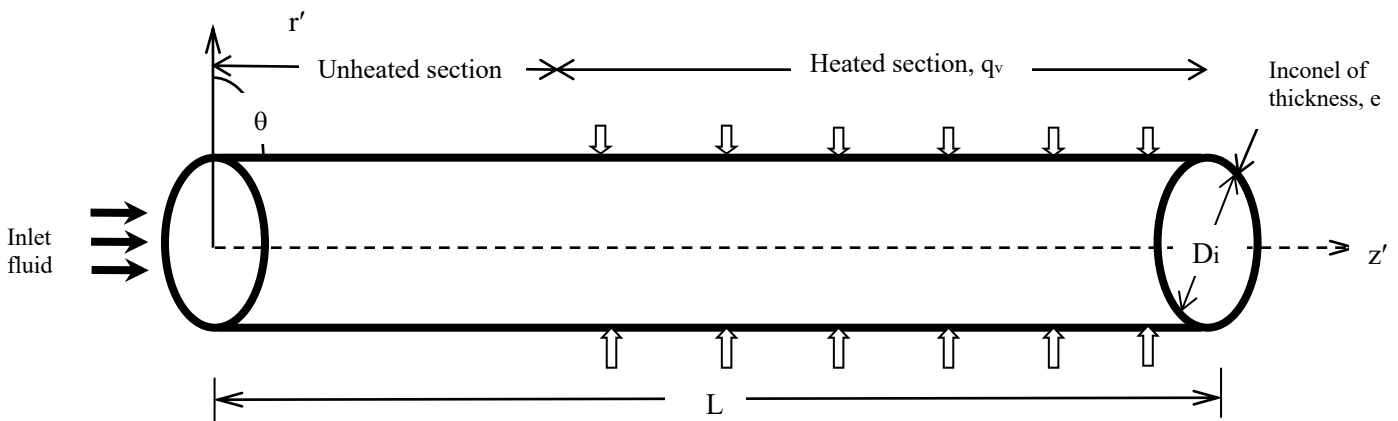


Fig. 1. Horizontal duct with boundary conditions.

2.2 Governing equations

By neglecting the viscous dissipation and using D_i , v_0 , ρv_0^2 , and $q_v D_i^2 / k_s$ as typical scales for

lengths, velocities, pressure, and temperature, the non-dimensional equations for a steady, three-dimensional, incompressible laminar flow with constant thermophysical properties, only the density was related with the temperature variation in the buoyancy terms [20], can be written as follows in cylindrical coordinate:

Continuity:

$$\frac{1}{r} \frac{\partial(ru)}{\partial r} + \frac{\partial v}{\partial z} + \frac{1}{r} \frac{\partial w}{\partial \theta} = 0 \quad (1)$$

r-Momentum:

$$\begin{aligned} u \frac{\partial u}{\partial r} + \frac{w}{r} \frac{\partial u}{\partial \theta} + v \frac{\partial u}{\partial z} - \frac{w^2}{r} = -\frac{\partial P}{\partial r} + \\ \frac{1}{\text{Re}} \left[\frac{1}{r} \frac{\partial}{\partial r} \left(r v^* \frac{\partial u}{\partial r} \right) + \frac{1}{r^2} \frac{\partial}{\partial \theta} \left(v^* \frac{\partial u}{\partial \theta} \right) + \frac{\partial}{\partial z} \left(v^* \frac{\partial u}{\partial z} \right) - \frac{u}{r^2} - \frac{2}{r^2} \frac{\partial w}{\partial \theta} \right] + \frac{\text{Gr}}{\text{Re}^2} \cos \theta \quad (2) \end{aligned}$$

z-Momentum:

$$\begin{aligned} u \frac{\partial v}{\partial r} + \frac{w}{r} \frac{\partial v}{\partial \theta} + v \frac{\partial v}{\partial z} = -\frac{\partial P}{\partial z} + \\ \frac{1}{\text{Re}} \left[\frac{1}{r} \frac{\partial}{\partial r} \left(r v^* \frac{\partial v}{\partial r} \right) + \frac{1}{r^2} \frac{\partial}{\partial \theta} \left(v^* \frac{\partial v}{\partial \theta} \right) + \frac{\partial}{\partial z} \left(v^* \frac{\partial v}{\partial z} \right) \right] \quad (3) \end{aligned}$$

θ -Momentum:

$$\begin{aligned} u \frac{\partial w}{\partial r} + \frac{w}{r} \frac{\partial w}{\partial \theta} + v \frac{\partial w}{\partial z} + \frac{uw}{r} = -\frac{1}{r} \frac{\partial P}{\partial \theta} + \\ \frac{1}{\text{Re}} \left[\frac{1}{r} \frac{\partial}{\partial r} \left(r v^* \frac{\partial w}{\partial r} \right) + \frac{1}{r^2} \frac{\partial}{\partial \theta} \left(v^* \frac{\partial w}{\partial \theta} \right) + \frac{\partial}{\partial z} \left(v^* \frac{\partial w}{\partial z} \right) - \frac{w}{r^2} - \frac{2}{r^2} \frac{\partial u}{\partial \theta} \right] - \frac{\text{Gr}}{\text{Re}^2} \sin \theta \quad (4) \end{aligned}$$

Energy equation:

$$u \frac{\partial \Theta}{\partial r} + \frac{w}{r} \frac{\partial \Theta}{\partial \theta} + v \frac{\partial \Theta}{\partial z} = \frac{1}{\text{RePr}} \left[\frac{1}{r} \frac{\partial}{\partial r} \left(r k^* \frac{\partial \Theta}{\partial r} \right) + \frac{1}{r^2} \frac{\partial}{\partial \theta} \left(k^* \frac{\partial \Theta}{\partial \theta} \right) + \frac{\partial}{\partial z} \left(k^* \frac{\partial \Theta}{\partial z} \right) \right] + S \quad (5)$$

where,

$$v^* = \begin{cases} \frac{v_f}{v_f} = 1 & \text{in the fluid zone} \\ v_f & \\ \frac{v_S}{v_f} \rightarrow \infty & \text{in the solid zone} \\ v_f & \end{cases} \quad k^* = \begin{cases} \frac{k_f}{k_f} = 1 & \text{in the fluid region} \\ k_f & \\ \frac{k_S}{k_f} = 25 & \text{in the liquid – solid interface} \\ k_f & \end{cases}$$

$$S = \begin{cases} 0 & \text{fluid region} \\ \frac{1}{\text{RePr}} k^* & \text{in the liquid – solid interface} \end{cases}$$

The Reynolds, Grashof and Prandtl numbers are defined, respectively, as : $Re = \frac{v_0 Di}{\nu}$, $Gr = \frac{g\beta \left(\frac{q_v Di^5}{k_s} \right)}{\nu^2}$,

$$Pr = \frac{\nu}{\alpha} .$$

2.3 Boundary conditions

The dimensionless boundary conditions of unheated and heated regions along the horizontal duct are:

- Fluid region:

At $z=0$ (inlet duct), $0 \leq r \leq 0.5$, $0 \leq \theta \leq 2\pi$: $u=0$, $v=2(1-4r^2)$, $w=0$, $\Theta=0$.

At $z=L/ Di =100$ (outlet duct), $0 \leq r \leq 0.5$, $0 \leq \theta \leq 2\pi$: $\frac{\partial u}{\partial z} = \frac{\partial v}{\partial z} = \frac{\partial w}{\partial z} = \frac{\partial}{\partial z} \left(k^* \frac{\partial \Theta}{\partial z} \right) = 0$

At $r=0$ (axis), $0 \leq \theta \leq 2\pi$, $0 \leq z \leq 100$, the dynamical axial conditions are considered and u , v , w , and Θ are correctly interpolated near the axis:

$$\frac{\partial}{\partial r} \left(\frac{\partial u}{\partial r} \right) = \frac{\partial}{\partial r} \left(\frac{\partial v}{\partial r} \right) = \frac{\partial}{\partial r} \left(\frac{\partial w}{\partial r} \right) = \frac{\partial}{\partial r} \left(\frac{\partial \Theta}{\partial r} \right) = 0$$

- Solid region:

At $0.5 \leq r \leq 0.52$, $0 \leq \theta \leq 2\pi$, $0 \leq z \leq 100$: $u=v=w=0$, $-k^* \frac{\partial \Theta}{\partial r} \Big|_{r=0.52} = \frac{(h_r + h)}{k_f} Di \Theta$

- Unheated region :

At $0.5 \leq r \leq 0.52$, $0 \leq \theta \leq 2\pi$, $0 \leq z \leq 25$: $u=v=w=0$, $\frac{\partial \Theta}{\partial r} = 0$

Where, h_r is the coefficient of radiative heat transfer, defined as [21] : $h_r = \sigma \epsilon (T^2 + T_\infty^2)(T + T_\infty)$, and h the coefficient of the convective heat transfer, $h=2.7W/m^2.K$ and the emissivity coefficient $\epsilon=0.9$.

2.4 Nusselt number

The local Nusselt number along the peripheral wall is:

$$Nu(\theta, z) = \frac{\frac{\partial \Theta}{\partial r} \Big|_{r=0.5}}{\Theta_w - \Theta_m(z)} \quad (7)$$

Where Θ_w and $\Theta_m(z)$ are the dimensionless wall and mean temperatures, respectively. $\Theta_m(z)$ is defined as follows:

$$\Theta_m(z) = \frac{\int_0^{0.5} \int_0^{2\pi} \Theta r dr d\theta}{\int_0^{0.5} \int_0^{2\pi} r dr d\theta} \quad (8)$$

The $Nu(z)$ peripherally averaged axial number is calculated by the integration of the local Nusselt number $Nu(\theta, z)$ along the heated wall:

$$Nu(z) = \frac{1}{2\pi} \int_0^{2\pi} Nu(\theta, z) d\theta \quad (9)$$

3. Numerical method and validation

3.1 Numerical method

The Finite-volume approach is used to solve the governing equations (1)-(5). The numerical procedure known as SIMPLER [22] is used to treat the coupling of pressure-velocity. The discretized algebraic equations are solved by the tridiagonal matrix algorithm (TDMA) line-by-line [22]. Convergence is confirmed when the maximal relative change falls below 10^{-5} for u , v , w , and Θ between two consecutive iteration levels.

3.2 Analysis of grid independence

In this work, three grids are used: $32 \times 82 \times 42$, $32 \times 162 \times 42$, and $32 \times 202 \times 42$ nodes. In the fluid, the non-uniform mesh is adopted in the radial and axial direction; the mesh is more refined in regions where the variations in velocity and temperature are important (At the inlet duct and the solid-fluid interface). In the wall of thickness e , five nodes have been chosen in the direction r . In the azimuthal direction, a uniform mesh was adopted. The values of $Nu(z)$ by using the grids $32 \times 162 \times 42$ and $32 \times 202 \times 42$ nodes are 10.98, respectively, for $Re=600$ and $Ri=2$. To maximize the processing time and cost of computations, the grid of $32 \times 162 \times 42$ nodes has been used. For the results presented here the total processor time on the workstation, *hp Z820* was around 10 h for each case.

3.3 Code validation

The FORTRAN code for mixed convection in a heated long circular duct was validated using experimental data from Abid et al.[1]. It should be noted that considered comparison [1] for temperature profiles at Grashof number $Gr=2.57 \times 10^5$ and Reynolds number $Re=143.28$. Figure 2 shows a good comparison of temperature at the top ($\theta=0$) and bottom ($\theta=\pi$) of the duct walls. Our results were compared with the experimental work of Barozzi *et al.* [23] and numerical data of Akbari *et al.* [24] at Rayleigh number $Ra=2.4 \times 10^4$ and $Re=200$. The obtained peripherally averaged local axial Nusselt number $Nu(z)$ in comparison with refs. [23] and [24] are illustrated in figure 3. As shown in figures 2-3, It is evident that our predictions are in excellent agreement with the references [1], [23] and [24].

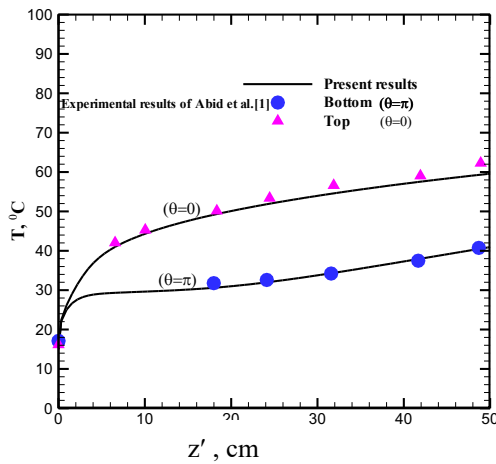


Fig. 2. Comparison of our numerical results and the Abid et al. experimental data[1].

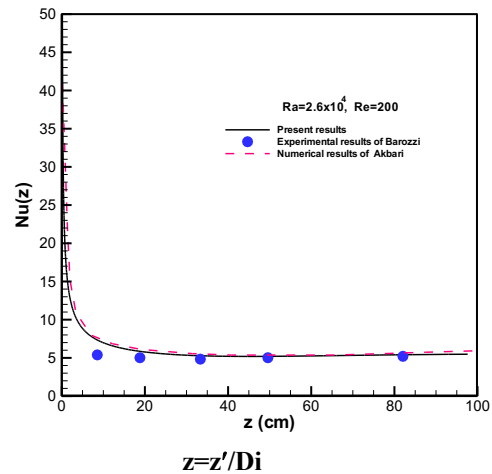


Fig. 3. Comparison of our results with those of Akbari et al.[24] and Barozzi et al.[23] experimental data.

4. Results and discussion

Results presented in this section are relative to numerical simulations carried out in mixed and forced convection in a horizontal cylindrical duct. The aspect ratio $L/D_i=100$ (where L is the duct length equal to 100cm and D_i its internal diameter $D_i=1$ cm). The Richardson number $Ri=Gr/Re^2$ is ranged between 0 and 8, which corresponds to Grashof number values $Gr=0$ and 2.88×10^6 and the Reynolds number is equal to $Re=10$ and 600. All results are presented in dimensionless form.

4.1 Reversed flow

Numerical simulations (see Figure 4) clearly show the influence of natural convection on the reversed flow, represented by velocity vectors in the r - z plane, at low Re and Gr numbers ($Re=10$ and $Gr=10^5$). For these values, forced convection is dominated by natural convection. The horizontal channel is composed of two zones: one unheated and the other heated. In the unheated zone ($0 \leq (z'/D_i)/10 \leq 2.5$), the imposed flow at the duct inlet is of Poiseuille type, only the axial velocity exists while the other components of the velocity are zero. In the heated zone ($2.5 < (z'/D_i)/10 \leq 4$), we see that near the upper wall, a part of the fluid is reversed (returned); velocity vectors take a direction opposite to that of the main flow (see, also Figure 5). This can be attributed to the importance of heat transfer by natural convection versus forced convection, which generates convective rolls. The heat transfer by natural convection is carried out from the hot fluid of the heated zone to the cold fluid of the unheated zone.

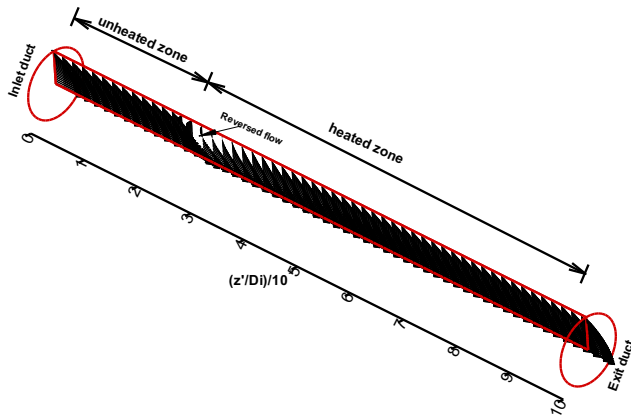


Fig. 4. Velocity vector field in the r - z plane along the horizontal duct, showing the reversed flow, for $Re=10$, $Gr=10^5$.

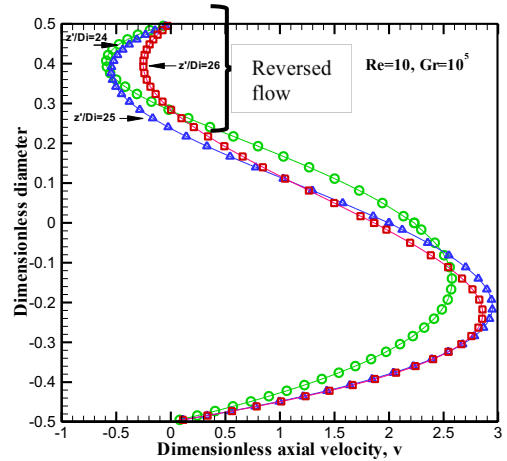


Fig.5. The axial velocity profiles v with the diameter of the tube, for various values of z'/D_i , showing the reversed flow (represented by negative values of the axial velocity near the top wall), at $Re=10$ and $Gr=10^5$.

4.2 Flow structure

For the case ($Ri=2$ and $Re=600$), the value of $z'/D_i=36$ corresponds to the hydrodynamic established zone, which agrees with the Abid et al. [1] experimental data. It should be noted that in the absence of heating in the zone ($0 \leq (z'/D_i)/10 \leq 2.5$), the flow profile is parabolic, imposed by the condition at the entrance of the duct, the maximum of which the dimensionless axial velocity $v=2$ is located at $r=0$, and the minimum at the wall (Figure 6). Upon entry of the heated zone, the flow represented by the transverse components (u - w) in the r - θ plane begins to grow gradually; the flow pattern consists of two convective rolls induced by natural convection (Figure 7). The existence of the secondary flow for $Ri=2$ and $Re=600$ is characterized by relatively low transverse velocities in comparison with that of the main flow, and contributes to the modification of the axial profile (Figure 6). It is visible in Figure 7 that there is a formation of two counter-rotating and symmetrical cells in the cross-section. Near the wall, the movement is upward while in the central area of the duct; it is

descending creating a counter-clockwise vortex: the less dense fluid particles will be pushed upwards. By symmetry, the flow follows the same path but in a clockwise direction. During the hydrodynamic establishment, one notices an increase in transverse velocities parallel to the dumping of the convective rolls; as z'/D_i increases, the convective rolls undergo compaction downwardly (Figure 7).

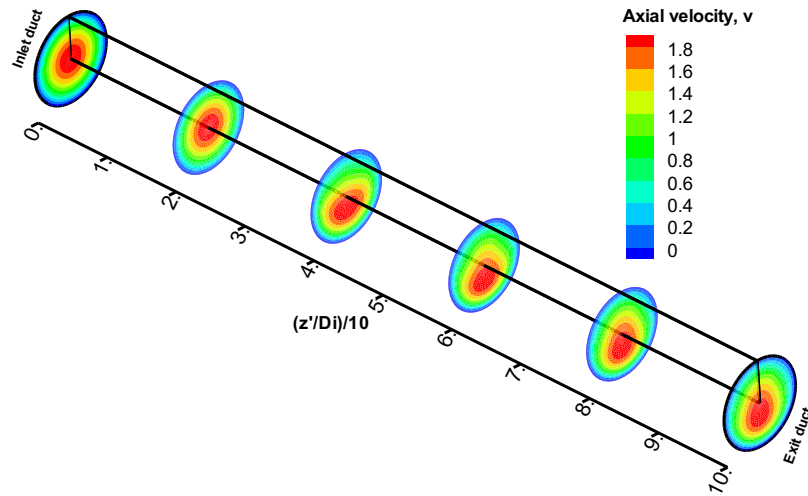


Fig.6. Contours of the axial velocity v for different values of z'/D_i , at $Ri = 2$ and $Re = 600$.

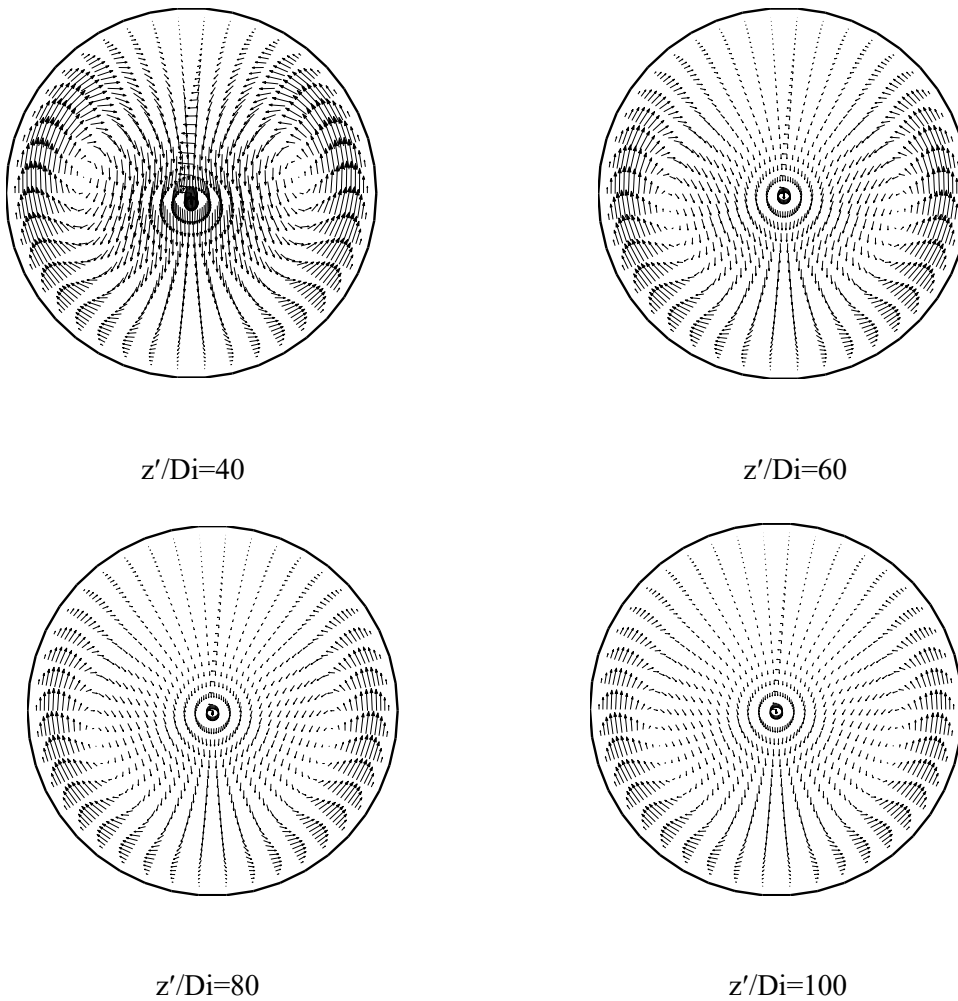


Fig. 7. Velocity vectors ($u-w$) in the plane $r-\theta$ for different values of z'/D_i (cross-section),

at $Ri = 2$ and $Re = 600$.

Figure 8 presents the profiles of the axial velocity v as a function of the diameter of the tube, for varying values of z'/Di at $Ri=Gr/Re^2=2$ and $Re=600$. The fluid accelerates in the central part of the section near the duct entrance. Subsequently, there is a slowing of the fluid as z'/Di increases until the duct exit. The parietal heating that accelerates the hot fluid at the wall may explain this slowing.

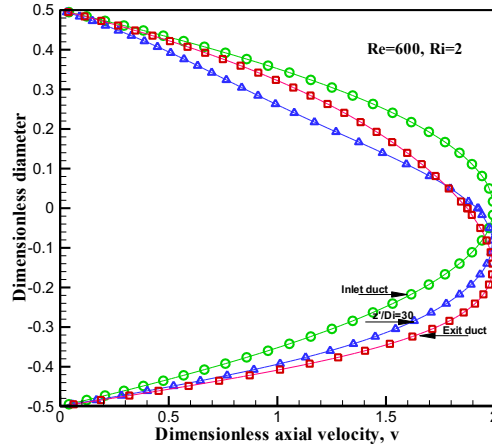


Fig. 8. Axial velocity profiles v with the diameter of the conduit, for different values of z'/Di at $Ri=Gr/Re^2=2$ and $Re=600$.

4.3 Thermal field

Figures 9a-b illustrate the thermal fields in the $r-\theta$ plane for two values of $Ri = 0.1$ and 2 and different z'/Di , at $Re = 600$. It is clear that in the unheated zone; isotherms are uniform, thus highlighting the absence of heat transfer between the fluid and the wall. On the other hand, in the heated zone, it is noted that the convective rolls disturb the isotherms along the duct. In the lower zone, the heat is transferred by the secondary flow to the upper zone of the cross-section. However, in the upper part of the transverse section, isotherms are almost horizontal (i.e. there is no thermal convection in the axial direction), evolving towards stratification of the flow. Similar results were observed in the works of Abid *et al.* [1] and [25]. This stratification occupies an increasingly important area. In a cross-section, the coldest zone of the fluid moves downward when z'/Di increases. The effect of Richardson number from 0.1 to 2 on the thermal field is clearly shown in Figure 9b; due to the contribution of natural convection.

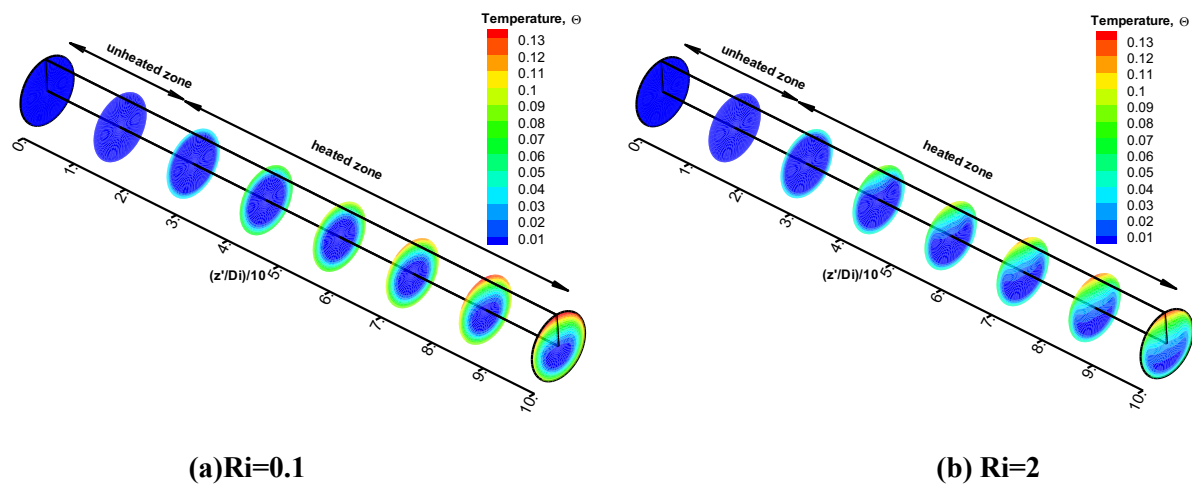


Fig. 9. Temperature fields for various values of z'/Di and Ri , at $Re = 600$.

Figure 10 displays the profiles of the temperature Θ in respect of the diameter of the tube, for three values of z'/Di at $Ri=2$ and $Re=600$. The values of these profiles show that the temperature in the upper zone increases with increasing z'/Di . This is highlighted by the temperature contours in a cross-section as shown in Figure 9.

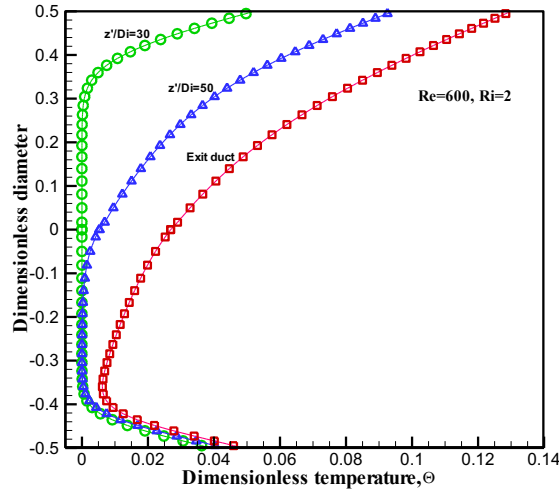


Fig.10. Profiles of the temperature Θ with the tube diameter, for various values of z'/Di at $Ri=2$ and $Re=600$.

4.4 Heat Transfer

The various obtained results allowed us to determine heat transfer coefficient. Thus, figure 11 illustrates the variation of $Nu(z)$ with z'/Di for different values of Ri , at $Re = 600$. We can notice that the hydrodynamics establishment zone varies according to Richardson number Ri . At $z'/Di = 25$, the $Nu(z)$ values are identical to those obtained by forced convection ($Ri=0$). We can see in this region that the peripherally averaged local axial Nusselt number decreases rapidly for different Richardson number values. This can be attributed to low natural convection activity coupled with thermal boundary layer formation. A significant impact of mixed convection on Nusselt number values is observed. In the region of hydrodynamic establishment, $Nu(z)$ takes an almost horizontal to the exit duct. The behavior was observed experimentally by Barozzi *et al.* [23] and numerically by Akbari *et al.* [24]. $Nu(z)$ values in mixed convection are greater than those obtained in forced convection (Fig. 11).

Figure 12 relates the variation of $Nu(z)$ as a function of z'/Di at $Ri=0$ (pure forced convection) and $Re = 600$. Here, the fluid is air and the value of our prediction $Nu(z)=4.43$, which is in very good agreement with that resulting from an analytical solution with constant surface heat flux ($Nu(z)=4.36$) [21].

Figure 13 displays the local Nusselt number $Nu(\theta,z)$, at $z'/Di = 80$, like a function of angular coordinate θ for various values of Ri ($Re = 600$) in the cross-section. The shape of $Nu(\theta,z)$ profiles is Gaussian. The values of $Nu(\theta,z)$ are maximum in $\theta=\pi$ (180°) and minimum in $\theta=0$ (0°), for the different Richardson numbers. To summarize the discussion of this figure, it can be said that the heat transfer increases sharply as one goes from top to bottom of the cross-section.

In the inlet region, a correlation for the variation of the peripherally averaged local axial Nusselt number average $Nu(Ri, z)$ on the heated wall based on the Richardson number and $z=z'/Di$ in a cross-section is proposed:

$$Nu(Ri, z) = 2390 Ri^{0.140} (z'/Di)^{-1.537} \quad (10)$$

And in the established zone, $z'/Di = 80$, another correlation for various Richardson number values is given as follow:

$$Nu(Ri) = 9.576 Ri^{0.71} \quad (11)$$

These two correlations (10) - (11) compared with the numerical results are illustrated in Figures 14 and 15, respectively. Figure 14 shows a slight difference between the numerical results and correlation, and a good agreement is observed in figure 15.

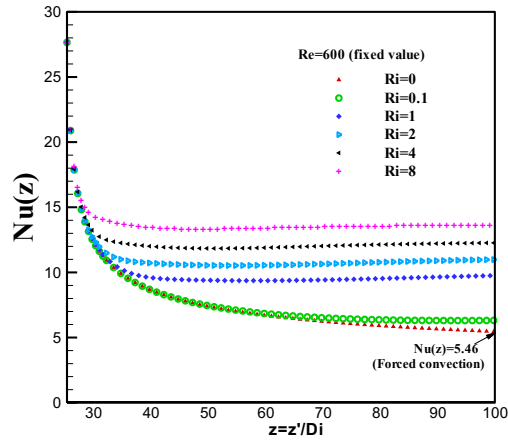


Fig. 11. Variation of $Nu(z)$ with z'/Di for various values of Ri , at $Re = 600$ (for water).

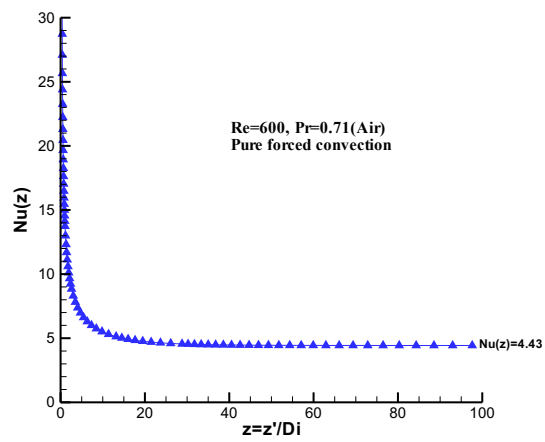


Fig. 12. Variation of $Nu(z)$ with z'/Di at $Ri=0$ and $Re = 600$ (for air).

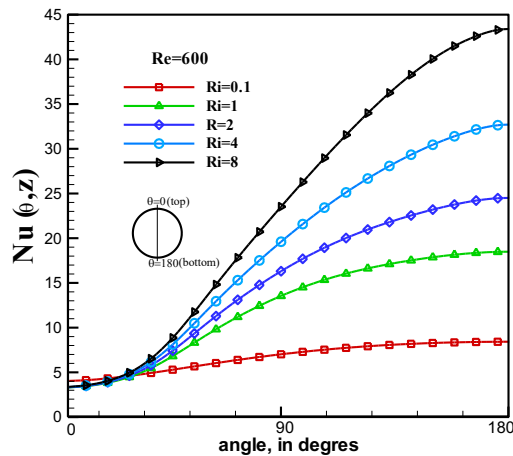


Fig.13. Variation of $Nu(\theta, z)$, at $z'/Di = 80$ (in the established zone), as a function of angular coordinate θ for different values of Ri , at $Re = 600$.

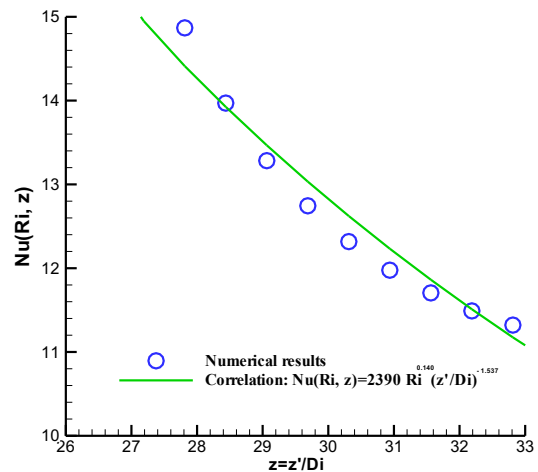


Fig.14. Variation of the peripherally averaged local axial Nusselt number $Nu(Ri, z)$ as a function of z'/Di in the entry zone: comparison between numerical results and correlation.

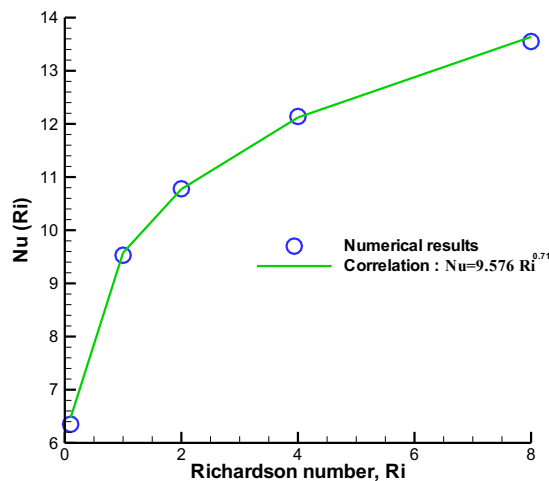


Fig. 15. Variation of Nu (Ri) with Ri in the established zone: comparison between numerical results and correlation.

5. Conclusion

In this paper, a numerical analysis was conducted of mixed convection in a horizontal cylindrical duct. We found the main following results:

- Reversed flow was observed at low Re, showing a natural convection effect on flow.
- Natural convection is causing a secondary flow, characterized by convective rolls.
- Secondary flow causes temperature gradient through a cross-section between the top and bottom of the duct.
- In the hydrodynamic establishment zone, the average values of the Nusselt number are higher than those obtained under forced convection.
- In mixed convection, the heat exchange between the fluid and the wall is better than forced convection.

References

- [1] C. Abid, F. Papini, A.Ropke, and D. Veyret, Etude de la convection mixte dans un conduit cylindrique. Approches analytique/numérique et détermination expérimentales de la température de paroi par thermographie infrarouge, *Int. J. Heat and Mass Transfer*, vol. 37, pp.91-101, 1994.
- [2] D.K. Choi and D.H. Choi, Developing mixed convection flow in a horizontal tube under circumferentially non-uniform heating, *Int. J. Heat and Mass Transfer*, vol. 37, pp.1899-1913, 1994.
- [3] G.J. Hwang and H.C. Lai, Laminar convective heat transfer in a horizontal isothermal tube for high Rayleigh numbers, *Int. J. Heat and Mass Transfer*, vol. 37, pp.1631-1640, 1994.
- [4] M. Ouzzane and N. Galanis, Effets de la conduction pariétale et de la répartition du flux thermique sur la convection mixte près de l'entrée d'une conduite inclinée, *Int. J. of Thermal Sciences*, vol. 38, pp.622-633, 1999.
- [5] M.A.Habib and A.A.A.Negm, Laminar mixed convection in horizontal concentric annuli with non-uniform circumferential heating, *Heat and Mass Transfer*, vol. 37, pp. 427-435, 2001.
- [6] J. Orfi and N. Galanis, Developing laminar mixed convection with heat and mass transfer in horizontal and vertical tubes, *Int. J. of Thermal Sciences*, vol. 41 pp.319-331, 2002.
- [7] J. Orfi and N. Galanis, Mixed convection with heat and mass transfer in horizontal tubes, *Int. Communications in Heat and Mass Transfer*, vol. 32 pp.511-519, 2005.
- [8] H. A. Mohammed and Y.K. Salman, Combined convection heat transfer for thermally developing aiding flow in an inclined circular cylinder with constant heat flux , *Applied Thermal Engineering*, vol. 27, pp.1236-1247, 2007.

- [9] H. A. Mohammed and Y.K. Salman, Free and forced convection heat transfer in the thermal entry region for laminar flow inside a circular cylinder horizontally oriented, *Energy Conversion and Management*, vol. 48, pp. 2185-2195, 2007.
- [10] H. A. Mohammed and Y.K. Salman, Combined natural and forced convection heat transfer for assisting thermally developing flow in a uniformly heated vertical circular cylinder, *Int. Communications in Heat and Mass Transfer*, vol. 34, pp. 474-491, 2007.
- [11] H. A. Mohammed and Y.K. Salman, Experimental investigation of mixed convection heat transfer for thermally developing flow in a horizontal circular cylinder, *Applied Thermal Engineering*, vol. 27, pp. 1522-1533, 2007.
- [12] H. A. Mohammed and Y.K. Salman, The effects of different entrance sections lengths and heating on free and forced convective heat transfer inside a horizontal circular tube, *Int. Communications in Heat and Mass Transfer*, vol. 34, pp.769-784, 2007.
- [13] H. A. Mohammed, The effect of different inlet geometries on laminar flow combined heat transfer inside a horizontal circular pipe, *Applied Thermal Engineering*, vol. 29, pp. 581-590, 2009.
- [14] B. Shiniyan, R. Hosseini, and H. Naderan, The effect of geometric parameters on mixed convection in an inclined eccentric annulus, *Int. J. Thermal Sciences*, vol. 68, pp. 136-147, 2013.
- [15] D.Testi, A novel correlation for azimuthal and longitudinal distributions of heat transfer coefficients in developing horizontal pipe flow under transitional mixed convection, *Int. J. Heat and Mass Transfer*, vol. 60, pp. 221-229, 2013.
- [16] M-S. Chae and B-J. Chung, Laminar mixed-convection experiments in horizontal pipes and derivation of a semi-empirical buoyancy coefficient, *Int. J. Thermal Sciences*, vol. 84, pp. 335-346, 2014.
- [17] T.M. Schriener, M.S. El-Genk, Convection heat transfer of NaK-78 liquid metal in a circular tube and a tri-lobe channel, *Int. J. Heat and Mass Transfer*, vol. 86, pp. 234-243, 2015.
- [18] L.P.M. Colombo, A. Lucchini, and A. Muzzio, Fully developed laminar mixed convection in uniformly heated horizontal annular ducts, *Int. J. of Thermal Sciences*, vol. 94, pp.204-220, 2015.
- [19] R. Ganesan, R. Narayanaswamy and K. Perumal, Mixed convection and radiation heat transfer in a horizontal duct with variable wall temperature, *Heat Transfer Engineering*, vol. 36, pp. 335-345, 2015.
- [20] A. Bejan, Convection Heat Transfer, 3rd edition, John Wiley and Sons, New-York, 2004
- [21] L. Bergman, S. Lavine, F. Incropera, and D. Dewitt, Fundamentals of Heat and Mass Transfer, 7th edition, John Wiley and Sons, USA, 2011.
- [22] S.V. Patankar, Numerical Heat Transfer and Fluid Flow, Hemisphere, Washington, DC, 1980.
- [23] G.S. Barozzi, E. Zanchini, and M. Mariotti, Experimental investigation of combined forced and free convection in horizontal and inclined tubes. *Meccanica*, vol. 20, pp. 18-27, 1985.
- [24] M. Akbari, A. Behzadmehr, and F. Shahraki, Fully developed mixed convection in horizontal and inclined tubes with uniform heat flux using nanofluid, *Int. J. Heat and Fluid Flow*, vol. 29, pp. 545-556, 2008.
- [25] C. Abid, R. Martin, and F. Papini, Thermal instabilities in a horizontal cylindrical duct: A physical approach, *Int. J. Heat and Mass Transfer*, vol. 45, pp.2153-2157, 2002.